Simultaneous biogas upgrading and centrate treatment in an outdoors pilot scale high rate algal pond

Esther Posadas[1], David Marín[1,3], Saúl Blanco[2], Raquel Lebrero[1], Raúl Muñoz*[1]

[1] Department of Chemical Engineering and Environmental Technology, Valladolid University, Dr. Mergelina, s/n, 47011, Valladolid, Spain.

[2] Department of Biodiversity and Environmental Management, University of León, 24071 León, Spain.

[3] Universidad Pedagógica Nacional Francisco Morazán, Boulevard Centroamérica, Tegucigalpa, Honduras.

* Corresponding author: mutora@iq.uva.es

ABSTRACT

The bioconversion of biogas to biomethane coupled to centrate treatment was evaluated in an outdoors pilot scale high rate algal pond interconnected to an external CO_2-H_2S absorption column (AC) via settled broth recirculation. CO_2-removal efficiencies ranged from 50 to 95% depending on the alkalinity of the cultivation broth and environmental conditions, while a complete H_2S removal was achieved regardless of the operational conditions. A maximum CH_4 concentration of 94% with a limited O_2 and N_2 stripping was recorded in the upgraded biogas at recycling liquid/biogas ratios in the AC of 1 and 2. Process operation at a constant biomass productivity of 15 g m^{-2} d^{-1} and the minimization of effluent generation supported high carbon and nutrient recoveries in the harvested biomass (C = 66±8%, N= 54±18%, P≈100% and S =16±3%). Finally, a low diversity in the structure of the microalgae population was promoted by the environmental and operational conditions imposed.

Keywords: algal-bacterial symbiosis, biogas upgrading, biomethane, microalgae, outdoors conditions, wastewater treatment.

1. Introduction

Biogas from the anaerobic digestion of organic solid waste and wastewater represents a renewable energy source with a significant potential to reduce the current world´s fossil fuel dependence (Hermann et al., 2016). Biogas can be used as a fuel for the on-site generation of domestic heat or steam and electricity in industry, as a substrate in fuel cells or as a substitute of natural gas prior upgrading (Andriani et al., 2014; Muñoz et al., 2015). For instance, the use of this biofuel in the European Union during 2014 supported a production of electricity and heat of 63.4 and 32.2 TWh, respectively (EBA, 2016). Biogas conversion to biomethane is highly recommended due to the high concentration of impurities present in the raw biogas: CO_2 (25-60%), CO (<0.6%), H_2S (0.005-2%), N_2 (0-2%), NH_3 (<1%), H_2O (5-10%), O_2 (0-1%), siloxanes (0-0.02%) and halogenated hydrocarbons (VOC <0.6%) (Ryckebosch et al., 2011). In fact, biogas upgrading is a mandatory step required prior biomethane injection into natural gas grids or use as a vehicle fuel, which must provide concentrations of CH_4 ≥95%, CO_2 ≤2%, O_2≤0.3% and negligible amounts of H_2S according to most international regulations (Muñoz et al., 2015). In this context, the removal of CO_2 from raw biogas would contribute to reduce the transportation costs and to increase the calorific value of biomethane, while the removal of H_2S would limit the corrosion in pipelines, boilers, engines, etc. (Posadas et al., 2015a).

Several physical-chemical and biological technologies are nowadays available at commercial scale to remove CO_2 and H_2S from biogas. Pressure swing adsorption, amine/water/organic scrubbing or membrane separation are typically applied to remove CO_2, while activated carbon filtration, chemical precipitation or anoxic/aerobic biotrickling filtration provide satisfactory levels of H_2S removal (Mann et al., 2016; Toledo-Cervantes et al., 2016; Muñoz et al., 2015). However, these H_2S and CO_2

52 removal technologies must be sequentially implemented to remove both biogas
53 contaminants, which makes physical-chemical biogas upgrading a costly and complex
54 two-stage process (Muñoz et al., 2015). The few technologies supporting a
55 simultaneous removal of CO_2 and H_2S from low S-strength biogas (i.e. chemical
56 scrubbing) exhibit high environmental impacts and operating costs (Tippayawong and
57 Thanompongchart, 2010). In this context, algal-bacterial photobioreactors have recently
58 emerged as an environmentally friendly and cost-efficient alternative to remove CO_2
59 and H_2S from raw biogas in a single step process (Bahr et al., 2014; Yan et al., 2016).

60 Photosynthetic biogas upgrading in algal-bacterial photobioreactors is based on the
61 simultaneous fixation of CO_2 by microalgae and oxidation of H_2S to SO_4^{2-} by sulfur
62 oxidizing bacteria or chemical reactions, the latter supported by the high dissolved
63 oxygen (DO) concentrations present in the cultivation broth (Posadas et al., 2015a;
64 Toledo-Cervantes et al., 2016). The economic and environmental sustainability of this
65 process can be boosted via integration of biogas upgrading with the recovery of
66 nutrients from digestate in the form of a valuable algal-bacterial biomass (Serejo et al.,
67 2015; Posadas et al., 2015a, 2016; Toledo-Cervantes et al., 2016; Yan et al., 2016).

68 Several investigations aiming at integrating photosynthetic biogas upgrading with
69 digestate treatment have been recently carried out in indoors high rate algal ponds
70 (HRAPs) interconnected to biogas absorption columns (AC) under artificial
71 illumination (Bahr et al. 2014; Alcántara et al., 2015; Posadas et al. 2015a, 2016; Serejo
72 et al. 2015; Meier et al. 2015; Toledo-Cervantes et al. 2016, 2017). Despite the rapid
73 optimization of this technology (Toledo-Cervantes et al., 2016, 2017), the constant
74 temperature (often in the optimum range) and irradiation (often too low compared to
75 solar irradiation) prevailing under laboratory conditions still hinder the complete
76 understanding of a process designed to be ultimately implemented outdoors under solar

irradiation. Therefore, the evaluation of the performance of photosynthetic biogas upgrading under outdoors conditions is crucial to understand the influence of the diurnal variations of light irradiance and temperature on the quality of the upgraded biogas. Similarly, process operation to minimize the desorption of O_2 and N_2 from the cultivation broth to the upgraded biogas, and to maximize nutrient recovery from digestates, must be optimized to the particular conditions prevailing during outdoors operation.

Despite the remarkable environmental advantages of using digestates as a nutrient source during biogas upgrading, their high nutrients content results in high biomass concentrations in the HRAPs (7-50 g L^{-1}) and the need to operate the process at low digestates flowrates. This severely decreases the photosynthetic efficiency of the system as a result of mutual shading and entails a net consumption of water to compensate evaporation losses (Posadas et al., 2016). In this context, all studies carried out to date set the make-up water input to maintain similar effluent and influent flowrates in order to guarantee a constant biomass output, which resulted in the generation of effluents with residual nutrient concentrations (Toledo-Cervantes et al., 2016; Posadas et al., 2016). On this basis, there is an urgent need to develop novel photobioreactor designs and operational strategies to minimize effluent generation while maintaining high microalgae productivities using digestates as a nutrient source.

This work aimed at evaluating the potential of a novel pilot scale HRAP interconnected to an AC via recirculation of the settled cultivation broth under outdoors conditions during the simultaneous upgrading of biogas and treatment of centrate. Process performance was evaluated under pseudo-steady state conditions at different alkalinity levels and make-up water supply regimes from June to October. Under each operational stage, process performance was also assessed during one diurnal cycle of temperature

and irradiance. A novel strategy decoupling biomass productivity from the effluent flowrate via control of the biomass wastage from the settler was applied to maximize the recovery of carbon and nutrients from biogas and centrate in the form of harvested biomass. Finally, the influence of the recycling liquid/biogas (L/G) ratio on the efficiency of biogas upgrading was also evaluated during a 24 h diurnal cycle.

2. Materials and methods

2.1 Biogas and centrate

A synthetic biogas mixture, composed of CO_2 (29.5%), H_2S (0.5%) and CH_4 (70%), was used as a model biogas (Abello Linde; Spain). Centrate was obtained from the centrifuges dehydrating the anaerobically digested sludge of Valladolid wastewater treatment plant and stored at 4 ºC prior to use. Centrate composition along the experimental period was subjected to the typical variations of real wastewaters: total organic carbon (TOC) = 70±8 mg L^{-1}, inorganic carbon (IC) = 522±40 mg L^{-1}, total nitrogen (TN) = 580±102 mg L^{-1}, $N\text{-}NH_4^+$ = 553±67 mg L^-, $P\text{-}PO_4^{3-}$ = 34±7 mg L^{-1} and SO_4^{2-} = 9±9 mg L^{-1}.

2.2 Experimental set-up

The pilot plant was located outdoors at the Department of Chemical Engineering and Environmental Technology of Valladolid University (41.39º N, 4.44º W). The experimental set-up consisted of a 180 L HRAP with an illuminated surface of 1.20 m^2 (length = 170 cm; width = 82 cm; depth =15 cm) and two water channels divided by a central wall and baffles in each side of the curvature. The HRAP was interconnected to an external 2.5 L bubble absorption column (internal diameter = 4.4 cm; height = 165 cm) provided with a metallic gas diffuser (2 μm pore size) located at the bottom of the column. The HRAP and AC were interconnected via external liquid recirculation of the supernatant of the algal-bacterial cultivation broth from an 8 L settler located at the

127 outlet of the HRAP (Fig. 1). The internal recirculation velocity of the cultivation broth
128 in the HRAP was ≈ 20 cm s^{-1}, which was provided by the continuous rotation of a 6-
129 blade paddlewheel.

130 **<Figure 1>**

131 **2.3 Operational conditions and sampling procedures**

132 Process operation was carried out from June 29th to October the 4th 2016. Based on a
133 previous study conducted by Norvill et al. (2017) in a similar HRAP treating urban
134 wastewater at 4 days of hydraulic retention time (HRT) in the same location, a constant
135 biomass productivity of 15 g m^{-2} d^{-1} was set throughout the 92 days of operation. The
136 required C, N and P input to maintain this biomass productivity was 9.7 g C d^{-1}, 1.9 g N
137 d^{-1} and 0.2 g P d^{-1}, assuming a C, N and P biomass content of 45, 9 and 1%, respectively
138 (Posadas et al., 2015b). This required a centrate flow rate of 3.2 L d^{-1} (considering an IC
139 and N-NH_4^+ stripping of 20%, and the absence of P removal by precipitation; Posadas et
140 al. (2013)) and a biogas flow rate of 74.9 L d^{-1} (assuming an average CO_2 removal
141 efficiency in the AC of 80% based on Posadas et al. (2015a)). The recycling
142 liquid/biogas (L/G) ratio in the AC was fixed at 0.5 according to Toledo-Cervantes et al.
143 (2016). The liquid and biogas residence time in the AC under these operational
144 conditions were 96 and 48 min, respectively. The settled biomass in the settler was
145 continuously recirculated to the HRAP at a flow rate of 7.2 L d^{-1}. This, together with the
146 external recycling, resulted in a HRT in the settler of 4.4 h. This process configuration
147 has been shown to increase the settleability of the algal-bacterial biomass, while
148 avoiding biomass degradation in the settler (Valigore et al., 2012; Park et al., 2011,
149 2013). Biomass harvesting was performed by daily removing the required settled
150 biomass volume according to its total suspended solids (TSS) concentration in order to
151 maintain the above mentioned biomass productivity.

The HRAP was initially filled with tap water (IC = 550 mg L^{-1}) and inoculated to an initial concentration of 210 mg TSS L^{-1} with *Chlorella* sp. from a HRAP treating centrate at the Department of Chemical Engineering and Environmental Technology of Valladolid University (Spain). The system was inoculated on June 29th, and after 5 d of inoculum acclimation batchwise, three different operational conditions were tested (corresponding to stages I, II and III) to optimize the simultaneous outdoors biogas upgrading and centrate treatment from a technical and environmental view point (Table 1).

<Table 1>

Stage I (reference state) was conducted at a centrate IC concentration of 522 ± 40 mg C L^{-1}. During stages II and III, the IC concentration of the centrate was increased up to 2024±124 mg C L^{-1} by addition of $NaHCO_3$ and Na_2CO_3, which increased the pH of the centrate from 8.38±0.33 in stage I to 9.94±0.09 and 10.06±0.13 in stages II and III, respectively (Table 1). Tap water was fed to the HRAP in stages I and II to compensate evaporation losses and maintain an effluent flowrate of 0.6±0.4 and 0.8±0.4 L d^{-1}, respectively, thus minimizing the loss of carbon, nutrients and fresh water. The effluent from the system was returned to the HRAP in stage III to minimize the supply of $NaHCO_3$ and Na_2CO_3, with a subsequent decrease in the supply of make-up water. Each operational stage was maintained for approximately one month, where temperature, solar irradiation and number of sun hours remained approximately constant (Table 1). The results obtained for the liquid phase throughout the three operational stages were provided as average values along with their corresponding standard deviation from measurements recorded for four consecutive days during each steady state.

The ambient and cultivation broth temperatures, influent and effluent flowrates, DO and pH in the cultivation broth, and the photosynthetic active irradiation (PAR) were daily

177 monitored. Gas samples of 100 µL of the raw and upgraded biogas were drawn twice a
178 week to monitor the concentrations of CO_2, H_2S, CH_4, O_2 and N_2. The inlet and outlet
179 biogas flowrates in the AC were also measured to accurately determine both CO_2 and
180 H_2S removals, and CH_4 losses by absorption. Liquid samples of 100 mL from the
181 centrate and the treated effluent after settling were withdrawn twice a week to monitor
182 the pH, TSS concentration, and concentrations of dissolved TOC, IC, TN, N-NH_4^+, N-
183 NO_2^-, N-NO_3^-, P-PO_4^{3-} and SO_4^{2-} following sample filtration through 0.20 µm nylon
184 filters. Likewise, liquid samples of 25 mL were drawn from the cultivation broth and
185 from the bottom of the settler twice a week to monitor the algal-bacterial TSS
186 concentration. The algal-bacterial biomass harvested from the settler under steady state
187 was washed three times with distilled water and dried for 24 hours at 105 ºC to
188 determine its elemental composition (C, N, P and S). Process monitoring and biomass
189 harvesting were always conducted at 9:00 a.m. along the entire experimental period.

190 At the end of each operational stage, the outdoors temperature and PAR, along with the
191 temperature, DO concentration and pH in the HRAP, settler and AC were measured
192 every 30 minutes during one entire diurnal cycle from one hour prior to dawn to one
193 hour after sunset. The composition and flowrate of the upgraded biogas were recorded
194 every hour, and the concentrations of TOC, IC and TN in the HRAP, settler and AC
195 were analyzed every 2 hours.

196 **2.4 Influence of the L / G ratio on the quality of the upgraded biogas**

197 L/G ratios ranging from 0.5 to 5 were tested at the end of stage III (4^{th} - 7^{th} October) to
198 optimize the quality of the upgraded biogas. A biogas flowrate of 74.9 L d^{-1} was
199 maintained while the liquid flowrates were set at 37.5, 74.9, 149.8 and 374.5 L d^{-1}
200 (providing L/ G ratios of 0.5, 1, 2 and 5, respectively). Each L/G ratio was maintained
201 for 12 h during one-day diurnal cycle. The ambient temperature and PAR, along with

the temperature, DO and pH in the HRAP, settler and AC, and the composition and flowrate of the upgraded biogas, were measured every two hours from one hour prior to dawn to one hour after sunset.

2.5 Analytical procedures

The monthly average ambient temperatures, PARs and number of sun hours were provided by the official AEMET meteorological station located at the University of Valladolid. CO_2, H_2S, CH_4, O_2 and N_2 gas concentrations were determined using a Varian CP-3800 GC-TCD (Palo Alto, USA) according to Posadas et al. (2015a). Temperature and DO concentration were determined using an OXI 330i oximeter (WTW, Germany). An Eutech Cyberscan pH 510 (Eutech instruments, The Netherlands) was used for pH determination. The PAR was measured with a LI-250A light meter (LI-COR Biosciences, Germany). The concentrations of dissolved TOC, IC and TN were measured using a Shimadzu TOC-VCSH analyzer (Japan) coupled with a TNM-1 chemiluminescence module. $N\text{-}NH_4^+$ concentration was determined with an ammonium specific electrode Orion Dual Star (Thermo Scientific, The Netherlands). The concentrations of $N\text{-}NO_3^-$, $N\text{-}NO_2^-$, $P\text{-}PO_4^{3-}$ and SO_4^{2-} were quantified by HPLC-IC according to Posadas et al. (2013). All analyses were carried out according to Standard Methods (APHA, 2005).

The determination of the C, N and S content of the algal-bacterial biomass was conducted in a LECO CHNS-932 analyzer, while phosphorus content was determined spectrophotometrically after acid digestion in a microwave according to Standard Methods (APHA, 2005). The identification, quantification and biometry measurements of the microalgae assemblage under steady state were performed by microscopic examination (OLYMPUS IX70, USA) of biomass samples (fixed with lugol acid at 5% and stored at 4 ºC prior to analysis) according to Sournia (1978).

3. Results and discussion

3.1. Environmental parameters

The average ambient temperature, PAR and number of sun hours slightly decreased from stage I (July) to stage III (September), which is inherent to outdoors environmental conditions in European latitudes (Table 1). Despite these variations, the environmental conditions were comparable throughout the three experimental stages and therefore the imposed operational conditions can be considered the main parameters influencing process performance.

The DO concentration, temperature and pH in the cultivation broth of the HRAP during a diurnal cycle at the end of each operational stage were directly correlated with the ambient temperature and light irradiance (Fig. A.1-A.4). Hence, the DO concentration in the HRAP during steady state in stages I, II and III fluctuated from 1.4 to 15.6, 1.3 to 16.7 and 0.9 to 13.2 mg O_2 L^{-1}, respectively (Fig. A.2). Microalgae activity was not inhibited at such low-moderate DO concentrations, since pernicious effects on photosynthesis are typically encountered above 25 mg O_2 L^{-1} (Molina et al., 2001). The average temperature and pH in the cultivation broth of the HRAP under steady state during stages I, II and III were 25±6, 25±6 and 19±5ºC, and 8.9±0.4, 10.0±0.0 and 9.9±0.0, respectively (Fig. A.3 and A.4). The higher pH recorded in stages II and III was attributed to the higher pH of the centrate fed to the system compared with that used during stage I. Moreover, the lower buffer capacity of the cultivation broth in this first operational stage (Table 1; Fig. A.5) resulted in significant variations of the pH along the day (from 8.3 to 9.4), which confirmed the key role of alkalinity for pH control in algal-bacterial photobioreactors (Posadas et al., 2013). The lower pH values recorded in the AC compared to those in the HRAP, regardless of the operational stage, were due to the acidification of the recycling broth caused by the absorption of CO_2 and

252 H_2S (Posadas et al., 2016) (Fig. A.4). Despite these sharp daily variations in
253 temperature, DO and pH, all parameters remained in the acceptable range to support
254 microbial activity (Posadas, 2016).

255 Finally, the evaporation rates during stages I, II and III accounted for 7±2 L, 9±1 and
256 3±2 L m^{-2} d^{-1}, respectively (Fig. A.6). The highest evaporation rate here recorded was
257 ~1.5 times higher than the maximum predicted for an arid area by Guieysse et al.
258 (2013). These high values were attributed to the high temperatures and turbulence in the
259 HRAP as a result of the typical oversizing of the motor of the paddlewheel in lab scale-
260 pilot systems (Posadas et al., 2015c; Guieysse et al., 2013). In this context, the scale-up
261 of this experimental set-up will likely entail lower evaporation rates.

262 **3.2 Biogas upgrading**

263 The composition of the biomethane obtained during stage I significantly varied
264 depending on the environmental conditions compared to stages II and III, where the
265 concentration of all biogas components remained approximately constant (Fig. 2). CH_4
266 concentrations in the upgraded biogas during stage I ranged from 72 to 93 %, while the
267 removal efficiencies (REs) of CO_2 and H_2S ranged from 50 to 75 % and from 91 to
268 100%, respectively. Average CH_4 concentrations of 90±2 % and 91±1 % were recorded
269 in the upgraded biogas during stages II and III, respectively, along with CO_2-REs of
270 86±4% and a complete H_2S removal regardless of the operational conditions (Fig. 2a).
271 These results also showed that the absence of effluent in stage III did not influence the
272 quality of the upgraded biogas. O_2 and N_2 concentrations in the biomethane during the
273 three operational stages ranged from 0.1 to 2.0% and from 0.6 to 5.0%, respectively,
274 depending on the pH of the cultivation broth and on the alkalinity (Fig. 2c). These
275 values were only slightly higher than those reported by Toledo-Cervantes et al. (2016)
276 during the indoors operation of a similar process at a L/G ratio of 1, which validated the

277 results obtained under laboratory conditions. CH_4 absorption in the AC was negligible,
278 with average losses of 2.2±1.2% (on a mass basis) along the three operational stages.
279 The biomethane composition obtained was both compliant with international
280 regulations for injection into natural gas grids in Europe (i.e. Belgium and The
281 Netherlands) and Latin-America (i.e. Chile), and suitable for use as autogas (Muñoz et
282 al., 2015).

283 **<Figure 2>**

284 The main fluctuations in the composition of the upgraded biogas were recorded during
285 stage I, which were attributed to the diurnal variations in irradiation and temperature. In
286 this context, the concentrations of CH_4, CO_2, H_2S, O_2 and N_2 in the upgraded biogas
287 ranged from 70.5 to 86.8%, 8.8 to 24.7%, 0 to 0.1%, 0.7 to 1.1% and 2.6 to 4.2%,
288 respectively, during the diurnal cycle evaluated in stage I (Fig. 3). The increase in the
289 alkalinity of the cultivation broth during stages II and III (from 267±56 mg IC L^{-1} in
290 stage I to 2174±253 and 2660±48 mg IC L^{-1} during stages II and III, respectively)
291 reduced the variability in the composition of the upgraded biogas. In this sense, CH_4,
292 CO_2, O_2 and N_2 concentrations in stage II ranged from 87 to 92%, 5 to 9%, 0 to 1% and
293 1 to 3%, respectively, while in stage III these concentrations varied from 85 to 93%, 4
294 to 12%, 0 to 2% and 1 to 3%, respectively (Fig. 3). H_2S was completely removed in
295 both stages.

296 The highest CO_2-REs, which entailed also the highest CH_4 concentrations in the
297 upgraded biogas, were recorded at the lowest ambient temperature regardless of the
298 operational stage as a result of the higher solubility of CO_2 (Sander, 1999). A 60%
299 decrease in CO_2 solubility is expected when temperature increases from 10 to 40°C
300 (Sander, 1999). However, the high CO_2 concentration gradient supported by the high
301 alkalinity of the cultivation broth in stages II and III compensated the decrease in CO_2

302 solubility mediated by the 30 °C temperature increase (Fig. A.3). The correlation
303 between the temperature of the cultivation broth in the settler and the CO_2 concentration
304 in the upgraded biogas was only significant during stage I. This result suggested that
305 CO_2 absorption in a low alkalinity media is controlled by the influence of the
306 temperature on the aqueous solubility of CO_2 (according to the Henry´s Law constant)
307 (Sander, 1999). However, the influence of the temperature on the concentration of O_2 or
308 N_2 in the upgraded biogas was negligible likely due to their limited aqueous solubility
309 (Fig. A.7). These results confirmed the high influence of the ionic strength of the
310 recycling cultivation broth on the quality of the upgraded biogas (Bahr et al. 2014). The
311 higher CO_2-REs recorded in stages II and III compared to stage I were likely mediated
312 by the pH increase in the cultivation broth, which significantly enhanced the CO_2
313 concentration gradient (Bahr et al. 2014; Toledo-Cervantes et al. 2016). The CO_2-REs
314 here reported were always higher than those recorded by Bahr et al. (2014) during
315 simultaneous biogas upgrading and centrate treatment (≈40%), and similar to those
316 obtained by Serejo et al. (2015), who reported an average CO_2-RE of ≈80% at a L/G
317 ratio of 10 during the upgrading of biogas combined with the treatment of diluted
318 anaerobically digested vinasse.

319 **<Figure 3>**

320 The high aqueous solubility of H_2S (three times higher than that of CO_2) resulted in
321 high H_2S-REs, comparable to those recorded in previous studies carried out under
322 laboratory conditions (Bahr et al., 2014; Posadas et al., 2015a; Serejo et al., 2015;
323 Toledo-Cervantes et al., 2016; Lebrero et al., 2016). A complete H_2S removal was
324 observed in stages II and III due to the higher pH of the cultivation broth (Fig. 2b),
325 which was in agreement with the results obtained by Bahr et al. (2014). H_2S oxidation
326 ratios (defined as the ratio between the mass of $S\text{-}SO_4^{2-}$ in the HRAP cultivation broth

and the mass of H_2S absorbed in the AC) of 36±13, 47±9 and 47±7 % were recorded during stages I, II and III, respectively. In this sense, an incomplete H_2S oxidation to SO_4^{2-} was also observed by Toledo-Cervantes et al. (2016) and Lebrero et al. (2016) likely due to the low O_2 concentration in the absorption column. Despite the fact that the highest DO concentrations were achieved during stage I, the lowest H_2S oxidation ratio recorded in this period was associated to the effect of the temperature on the solubility of the H_2S in a low ionic strength medium and therefore, to the limited H_2S mass transfer efficiency from the biogas to the liquid phase.

3.3 Influence of the L/G ratio on the quality of the upgraded biogas

The similar PAR and outdoor temperatures recorded during the five consecutive days of this study allowed an unbiased comparison of the influence of the L/G ratio on biomethane composition (Fig. A. 8). In fact, similar DO concentrations and temperature profiles were recorded in the HRAP regardless of the tested L/G ratio (Fig. A. 9), although the pH of the cultivation broth in the HRAP and AC varied depending on the L/G ratio tested (Figs. A.9-A.11). Thus, the daily average pH of the cultivation broth in the AC was 8.8±0.1, 9.4±0.1, 9.6±0.1 and 9.8±0.8 at L/G ratios of 0.5, 1, 2 and 5, respectively (Fig. A.10). This pH increase at higher L/G ratios was attributed to the lower CO_2 transferred per volume of recycling cultivation both, which prevented the acidification of the broth in the AC.

<Figure 4>

L/G ratios > 1 supported a significant decrease in CO_2 concentration in the upgraded biogas, which ranged from 1.8 to 3.7% and corresponded to CO_2-REs ≈ 95% (Fig. 4b). The increase in pH in the cultivation broth of the AC at increasing L/G ratios supported higher CO_2 concentrations gradient between the biogas and liquid phase, which enhanced CO_2-REs (Posadas et al., 2016). In our particular study, the maximum CO_2

mass transfer capacity was achieved at a L/G ratio of 1. In this context, Serejo et al. (2015) recorded a maximum CO_2 mass transfer (CO_2-RE of 95±2%) at a L/G ratio of 15, pH of 8 and IC concentrations ≈80 mg L^{-1}, respectively. On the other hand, Toledo-Cervantes et al. (2016) recorded a CO_2-RE of 98.8±0.2% regardless of the tested L/G (0.5-60) at a pH of 10 and IC concentration ≈4000 mg L^{-1}. These studies confirmed the key role of the alkalinity of the recycling cultivation broth on the biogas upgrading efficiency compared to other operational parameters.

H_2S was completely removed regardless of the tested ratio likely due to its high aqueous solubility (Bahr et al., 2014; Serejo et al., 2015). The O_2 and N_2 concentration in the upgraded biogas only increased significantly at a L/G ratio of 5 (up to 5.5% and 12.8%, respectively) (Fig. 4c, 4d). Indeed, the increase in the L/G ratio mediated a higher desorption of O_2 and N_2 from the recycling, which negatively impacted the final concentration of CH_4 in the upgraded biogas. In this context, the maximum CH_4 concentration (94%) was obtained at L/G ratios of 1 and 2 (Fig. 4a).

3.4 Wastewater treatment performance

The wastewater treatment efficiency of the HRAP was evaluated under pseudo-steady state at the three operational stages evaluated (Fig. 5; Figs. A12-A13).

<Figure 5>

The TOC effluent concentrations, which ranged from14 to 85 mg L^{-1}, were similar to the influent TOC concentrations due to the low biodegradability of the centrate, the concentration effect caused by the high water evaporation rates in the HRAP and the low or negligible effluent flowrates (Posadas et al., 2013; 2015c) (Fig. 5a). Despite the low DO concentrations recorded in the cultivation broth (<2 mg O_2 L^{-1}) in the early morning could have partially limited organic matter oxidation (Metcalf and Eddy,

2003), the removals of TOC estimated by mass balance calculations ranged from 59±7% (stage III) to 74±7% (stage I) (Table 2) (Fig. A.3).

<Table 2>

The TIC-REs in stage I were higher than those recorded in stages II and III as a result of the higher inorganic carbon feeding and C-CO_2 REs in the AC during these latter stages (Table 2). Therefore, only 65±6 and 66±8% of the total carbon removed in stages II and III was recovered in the harvested biomass, while a 97±1% carbon recovery was observed during stage I (Table 3). Despite the higher pH values should have promoted lower IC removals by stripping based on the limited CO_2 aqueous equilibrium concentration, the lower IC loading during stage I resulted in a lower fraction of C removed by stripping (Table 3) (Posadas et al., 2013) (Fig. 5b).

Similar TN-REs of 86±4, 87±4 and 80±4% were recorded during stages I, II and III, respectively, while a complete N-NH_4^+ removal occurred during the entire experimental period (Table 2; Fig. 5c, 5d). Nitrification was not inhibited by the high pH values prevailing during stages II and III or the low DO concentrations (<1 mg O_2 L^{-1}) present in the first hours in the morning (Fig. A.3). N-NO_2^- concentrations were low compared to N-NO_3^- despite temperatures higher than 28ºC were always recorded close to midday, which are known to promote the partial oxidation of N-NH_4^+ (Fig. 5e; Figs. A.2-A.3) (Metcalf and Eddy, 2003). The oxidation ratios (referred to [N-NO_3^-+ N-NO_2^-] mass outputs compared to TN mass input, Posadas et al. (2015a)) were 11±2, 13±4 and 19±8% during stages I, II and III, respectively. The high nitrification activity, together with the high evaporation rates, induced an increase in N-NO_3^- concentration in the cultivation broth up to 148 mg L^{-1} in stage I, 198 mg L^{-1} in stage II and 293 mg L^{-1} in stage III, this latter increase mediated by the absence of effluent from the HRAP (Fig. 5f). The nitrogen recovered in the harvested biomass accounted for 65±3, 54±18 and

401 76±19% of the total nitrogen removed during stages I, II and III, respectively (Table 3).
402 These values were considerably higher than those recorded by Posadas et al. (2015a)
403 (45±7%) and Toledo-Cervantes et al. (2017) (19±13% and 36±18%) in a similar indoors
404 experimental set-up during the simultaneous treatment of biogas and digestates as a
405 result of the lower microalgae productivities in those studies.

406 **<Table 3>**

407 High P-PO_4^{3-} REs of 92±2, 84±5 and 85±5% were recorded during stages I, II and III,
408 respectively (Table 2). The higher P-RE in stage I was likely mediated by the higher P
409 content of the harvested biomass (Table 3). In this regard, P-PO_4^{3-} concentration in the
410 cultivation broth increased up to 6 mg L^{-1} in stage I, 15 mg L^{-1} in stage II and 17 mg L^{-1}
411 in stage III. These increasing P-PO_4^{3-} concentration were also supported by the
412 evaporation rate and the low or negligible effluent flowrates (Fig. 5g). A P mass balance
413 revealed than approximately 100% of the P removed was recovered in the harvested
414 biomass, despite high pH values are known to promote PO_4^{3-} precipitation (Cai et al.,
415 2013) (Table 3).
416 Finally, H_2S oxidation supported an increase in SO_4^{2-} concentration in the cultivation
417 broth of the HRAP from 60 to 495 mg L^{-1} through the 92 operational days, also
418 triggered by the high evaporation rates and low effluent flowrates (Fig. 5h). The fraction
419 of H_2S not fully oxidized to sulphate would have remained as S-intermediates in the
420 liquid phase (S^o, thiosulfate or sulfite) (Toledo-Cervantes et al., 2016). This was
421 confirmed by the observation of S^o accumulation on the walls and diffuser of the AC
422 during stage I (Photograph 1, appendix), while a S mass balance revealed that only
423 26±5, 17±3 and 16±3% of the S removed was recovered in the harvested biomass
424 during stages I, II and III, respectively (Table 3). Further analyses to determine the
425 actual sulfur compounds present in the cultivation broth are required.

3. 5 Concentration and composition of the algal-bacterial biomass

The steady state biomass concentrations in the HRAP during stages I, II and III averaged 660±17, 1078±84 and 665±79 mg TSS L^{-1} (Fig. A. 14). The operational strategy here evaluated based on the control of biomass productivity via regulation of the settled biomass wastage rate successfully maintained the concentration of algal-bacterial biomass below light limiting values. At this point it should be stressed that the theoretical biomass concentration generated based on the centrate composition would be ≈2000 mg TSS L^{-1} (with P as the limiting nutrient). The good settling characteristics of the algal-bacterial (supporting TSS-REs in the settler of 80±9%) were likely promoted by the short HRT in the settler and the continuous recirculation of the settled biomass, which boosted the enrichment of rapidly settling algal-bacterial flocs (Valligore et al., 2011; Park et al., 2011).

The elemental composition of the harvested biomass remained within the typical range reported in literature, regardless of the operational stage (Posadas et al., 2016; Bi et al., 2013). C, N and P content in the biomass decreased from stage I to stage II and slightly increased in stage III (Table 3). The different C/N/P (g/g/g) ratios present in the cultivation broth of the HRAP (100/39/2, 100/6/1 and 100/12/1 during stages I, II and III, respectively) could have influenced this final biomass composition, despite the C/N ratio in the harvested biomass remained always at the optimum value of 6 regardless of the operational conditions (Serejo et al., 2015). The main differences were recorded in the S content, which decreased from 0.4% in stage I to 0.2% in stages II and III (Table 3). The higher S content in the biomass was recorded concomitantly with the occurrence of S precipitation (Photograph 1, appendix), and was attributed to the likely S absorption into the biomass.

450 The inoculated *Chlorella* sp. was gradually replaced by *Chloroidium saccharophilum*s
451 (*Chlorella saccharophila)* during stage I. *Chloroidium saccharophilum* was the
452 dominant microalga species during stage I (94%) and stage III (100 %), while
453 *Pseudanabaena* sp. accounted for 6% and 54% of the total number of microalgae cells
454 in stages I and II, respectively (Fig. 6). *Pseudanabaena* sp. has been consistently found
455 in a similar indoors experimental set-up during the simultaneous upgrading of biogas
456 and digested vinasse treatment (Posadas et al. 2015a; Serejo et al. 2015). The lower
457 microalgae diversity recorded outdoors compared to that observed under laboratory
458 conditions in a similar experimental set-up was likely due to i) the recirculation of the
459 settled biomass and ii) the high alkalinity in the cultivation broth in stages II and III
460 (Serejo et al., 2015; Posadas et al., 2015a; Toledo-Cervantes et al., 2016, 2017; Park et
461 al., 2011).

462 **<Figure 6>**

463 **4. Conclusions**

464 This work constitutes the first proof-of-concept study of photosynthetic biogas
465 upgrading coupled with centrate treatment at pilot scale under outdoors conditions. The
466 feasibility of a zero-effluent process operation was also demonstrated. Temperature
467 played a key role on the efficiency of biogas upgrading at low-to-medium alkalinities,
468 while high alkalinities enhanced process robustness against daily temperature
469 variations. Process operation at L/G ratios of 1-2 provided a biomethane complying
470 with most international regulations. A consistent centrate treatment was achieved
471 regardless of the operational conditions, while the decoupling of biomass productivity
472 from the HRT allowed high recoveries of C, N and P.

473 **ACKNOWLEGMENTS**

This research was supported by MINECO and the European Union through the FEDER program (CTM2015-70442-R and Red Novedar), the Regional Government of Castilla y León (Project VA024U14 and UIC 71) and INIA (RTA2013-00056-C03-02). The authors wish to thanks Julia Bilbao and Argimiro de Miguel from the Atmosphere and Energy Laboratory at Valladolid University for kindly providing the temperature, radiation data and number of sun hours. Valladolid University is also acknowledged for funding the research contract of Esther Posadas.

REFERENCES

(1) Alcántara C., García-Encina P., Muñoz R., 2015. Evaluation of simultaneous biogas upgrading and treatment of centrates in a HRAP through C, N and P mass balances. Water Sci. Technol. 72, 150-157.

(2) Andriani D., Wresta A., Atmaja T., Saepudin A., 2014. A review on optimization production and upgrading biogas through CO_2 removal using various techniques. Appl. Biochem. Biotechnol. 172, 1909–1928.

(3) APHA; AWWA; WEF. Standard Methods for the Examination of Water and Wastewater; 21st ed.; Washington, 2005.

(4) Bahr M., Díaz I., Domínguez A., González Sánchez A., Muñoz R., 2014. Microalgal-biotechnology as a platform for integral biogas upgrading and nutrient removal from anaerobic effluents. Environ. Sci. Technol. 48, 573-581.

(5) Bi Z., He B. B., 2013. Characterization of microalgae for the purpose of biofuel production, Transactions of the ASABE, Vol. 56 (4), 1529-1539.

(6) Cai T., Park S.Y., Li Y., 2013. Nutrient recovery from wastewater streams by microalgae: Status and prospects. Renew. Sust. Energ. Rev. 19, 360-369.

(7) European Biogas Association (EBA): ATBEST International Conference 7-8 September (2016), Linköping by Arthur Wellinger.

(8) Guieysse B., Béchet Q., Shilton A., 2013. Variability and uncertainty in water demand and water footprint assessments of fresh algae cultivation based on case studies from five climatic regions. Bioresour. Technol. 128, 317–323.

(9) Herrmann C., Kalita N., Wall D., Xia A., Murphy J. D., 2016. Optimised biogas production from microalgae through co-digestion with carbon-rich co-substrates. Bioresour. Technol. 214, 328-337.

(10) Lebrero R., Toledo-Cervantes, Muñoz R., Del Nery V., Foresti E., 2016. Biogas upgrading from vinasse digesters: a comparison between ananoxic biotrickling filter and an algal-bacterial photobioreactor. J. Chem. Technol. Biotechnol. 91 (9), 2488-2495.

(11) Mann G., Schlegel M., Kanswohl N., Schumann R., 2016. Experimental system for the prevention of O_2– and air contamination during biogas upgrading with phototrophic microalgae. Appl Agric Forestry Res. DOI: 10.3220/LBF1471268642000.

(12) Meier L., Pérez R., Azócar L., Rivas M., Jeison D. 2015. Photosynthetic CO_2 uptake by microalgae: an attractive tool for biogas upgrading. Biomass and bioenergy, 73, 102-109.

(13) Metcalf, Eddy, 2003. Wastewater Engineering and Reuse, 4th ed., New York, Mc. GrawHill.

(14) Molina E., Fernández J. M., Acién F. G., Chisti Y., 2001. Tubular photobioreactors design for algal cultures. J. Biotechnol. 92, 113-131.

(15) Muñoz R., Meier L., Díaz I, Jeison D., 2015. A review on the state-of-the-art of physical/chemical and biological technologies for biogas upgrading. Rev. Environ. Sci. Biotechnol. 14, 727–759.

(16) Norvill Z., Toledo-Cervantes A., Blanco S., Shilton A., Guieysse B., Muñoz R., 2017. Photodegradation and sorption govern tetracycline removal during wastewater treatment in algal ponds. Bioresource Technology (submitted for publication).

524 (17) Park J.B.K., Craggs R.J., Shilton A.N., 2013. Enhancing biomass energy yield
525 from pilot-scale high rate algal ponds with recycling. Water Res. 47 (13), 4422-4432.
526 (18) Park J.B.K., Craggs R.J., Shilton A.N., 2011. Recycling algae to improve
527 species control and harvest efficiency from a high rate algal pond. Water Res. 45 (20),
528 6637-6649.
529 (19) Posadas, 2016. Innovative algal-bacterial processes for wastewater treatment: a
530 further step towards full scale implementation:
531 http://uvadoc.uva.es/handle/10324/18777.
532 (20) Posadas E., García-Encina P. A., Soltau A., Domínguez A., Díaz I., Muñoz R.,
533 2013. Carbon and nutrient removal from centrates and domestic wastewater using algal-
534 bacterial biofilm bioreactors. Bioresour. Technol. 139, 50-58.
535 (21) Posadas E., Morales M. M., Gómez C., Acién F. G., Muñoz R., 2015b. Influence
536 of pH and CO_2 source on the performance of microalgae-based secondary domestic
537 wastewater treatment in outdoors pilot raceways. Chem. Eng. J. 265, 239-248.
538 (22) Posadas E., Muñoz A., García-González M.-C., Muñoz R., García-Encina P. A.,
539 2015c. A case study of a pilot high rate algal pond for the treatment of fish farm and
540 domestic wastewaters, J. Chem. Technol. Biotechnol. 90 (6), 1094-1101.
541 (23) Posadas E., Serejo M., Blanco S., Pérez R., García-Encina P.A., Muñoz R.,
542 2015a. Minimization of biomethane oxygen concentration during biogas upgrading
543 inalgal–bacterial photobioreactors. Algal Res. 12, 221-229.
544 (24) Posadas E., Szpak D., Lombó F., Domínguez A., Díaz I., Blanco S., García-
545 Encina P., Muñoz R., 2016. Feasibility study of biogas upgrading coupled with nutrient
546 removal from anaerobic effluents using microalgae-based processes. J. Appl. Phycol. 28
547 (4), 2147-2157.

548 (25) Ryckebosch E., Drouillon M., Vervaeren H., 2011.Techniques for
549 transformation of biogas to biomethane. Biomass. Bioenerg. 35 (5), 1633-1645.
550 (26) Sander R., 1999. Compilation of Henry's Law Constants for Inorganic and
551 Organic Species of Potential importance in Environmental Chemistry (Last access:
552 30.11.2016): http://www.mpchmainz.mpg.de/sander/res/henry.html
553 (27) Serejo M., Posadas E., Boncz M., Blanco S., Garcia-Encina PA., Muñoz R.,
554 2015. Influence of biogas flow rate on biomass composition during the optimization of
555 biogas upgrading in microalgal-bacterial processes. Environ. Sci. Technol. 49 (5), 3228-
556 3236.
557 (28) Sournia A., Phytoplanton Manual. Museum National d' Historie Naturelle, París,
558 United Nations Educational, Scientific and Cultural Organization (Unesco), 1978.
559 (29) Toledo-Cervantes A., Madrid-Chirinos C., Cantera S., Lebrero R., Muñoz R.,
560 2017. Influence of the gas-liquid flow configuration in the absorption column on
561 photosynthetic biogas upgrading in algal-bacterial photobioreactors. Bioresour.
562 Technol., 225, 336-342.
563 (30) Toledo-Cervantes A., Serejo M., Blanco S., Pérez R., Lebrero R., Muñoz R.,
564 2016. Photosynthetic biogas upgrading to bio-methane: Boosting nutrient recovery via
565 biomass productivity control. Algal Res., 17, 46-52.
566 (31) Tippayawong N., Thanompongchart P., 2010: Biogas quality upgrade by
567 simultaneous removal of CO_2 and H_2S in a packed column reactor. Energy 35 (12),
568 4531-4535.
569 (32) Valigore J. M., Gostomski P. A. , Wareham D. G. , O'Sullivan A. D., 2012.
570 Effects of hydraulic and solids retention times on productivity and settleability of
571 microbial (microalgal-bacterial) biomass grown on primary treated wastewater as a
572 biofuel feedstock. Water Res. 46, 2957-2964.

573 (33) Yan C., Muñoz R., Zhu L., Wang Y. (2016). The effects of various LED (light
574 emittion diode) lighting strategies on simultaneous biogas upgrading and biogas slurry
575 nutrient reduction by using of microalgae Chlorella sp. Energy 106, 554-561.

576 **FIGURE CAPTIONS**

577 **Figure 1.** Schematic diagram of the outdoors experimental set-up used for the
578 continuous upgrading of biogas.

579 **Figure 2.** Time course of the concentration of (a) CH_4 (■), (b) CO_2 (♦) and H_2S (▲),
580 and (c) O_2 (●) and N_2 (○) in the upgraded biogas. The removal efficiencies of CO_2 (◊)
581 and H_2S (Δ) are also displayed in figure 2b.

582 **Figure 3.** Time course of the concentration of (a) CH_4, (b) CO_2, (c) O_2 and (d) N_2 in the
583 upgraded biogas during the one-day cycle evaluated in stages I (♦), II (■) and III (▲).

584 **Figure 4.** Time course of the concentration of (a) CH_4, (b) CO_2, (c) O_2 and (d) N_2 in the
585 upgraded biogas at L / G ratios of 0.5 (♦), 1 (□), 2 (▲) and 5 (○).

586 **Figure 5.** Time course of the influent (♦) and effluent (◊) concentrations of (a) TOC, (b)
587 IC, (c) TN, (d) $N\text{-}NH_4^+$, (e) $N\text{-}NO_2^-$, (f) $N\text{-}NO_3^-$, (g) $P\text{-}PO_4^{3-}$ and (h) SO_4^{2-} throughout
588 the three operational stages.

589 **Figure 6.** Time course of the structure of microalgae population in the HRAP: (■)
590 *Chlorella* sp., (▩) *Pseudanabaena* sp. and (□) *Chloroidium saccharophilum*.

Figure
Click here to download Figure: Figure 1.docx

Figure 1. Schematic diagram of the outdoors experimental set-up used for the continuous upgrading of biogas.

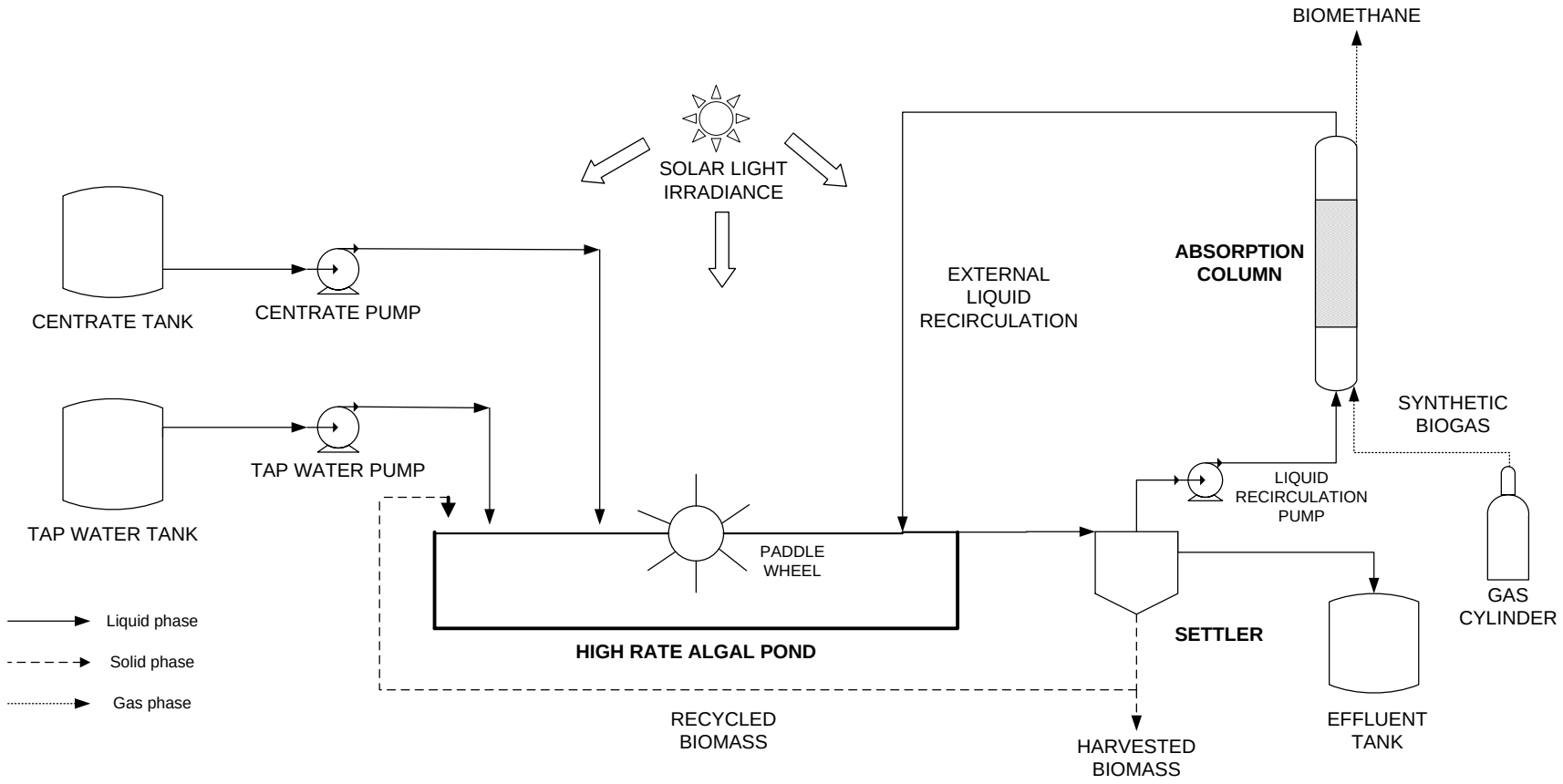

Figure
Click here to download Figure: Figure 2.docx

Figure 2. Time course of the concentration of (a) CH_4 (■), (b) CO_2 (♦) and H_2S (▲), and (c) O_2 (●) and N_2 (○) in the upgraded biogas. The removal efficiencies of CO_2 (◊) and H_2S (Δ) are also displayed in figure 2b.

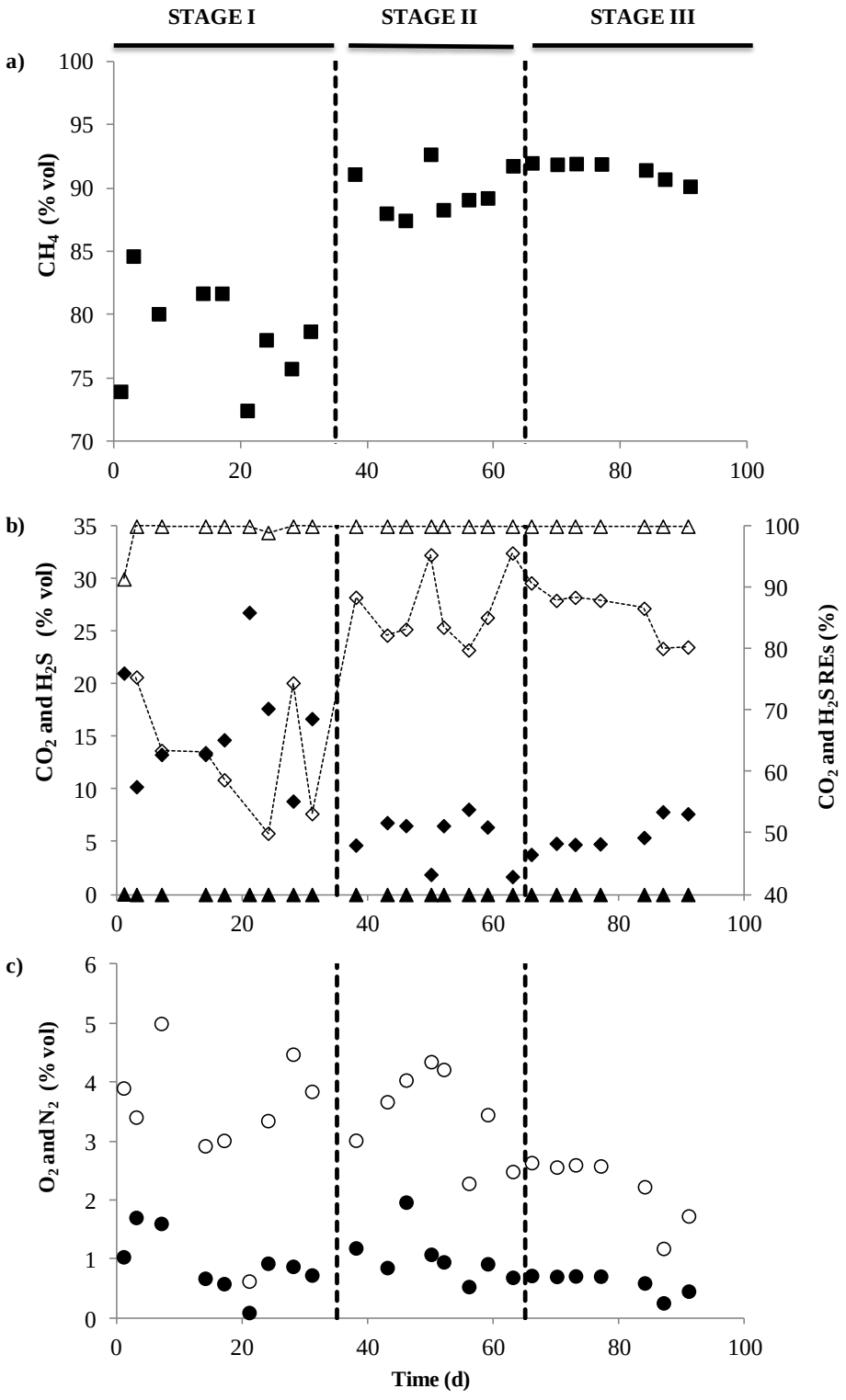

Figure
Click here to download Figure: Figure 3.docx

Figure 3. Time course of the concentration of (a) CH_4, (b) CO_2, (c) O_2 and (d) N_2 in the upgraded biogas during the diurnal cycle evaluated in stages I (♦), II (■) and III (▲).

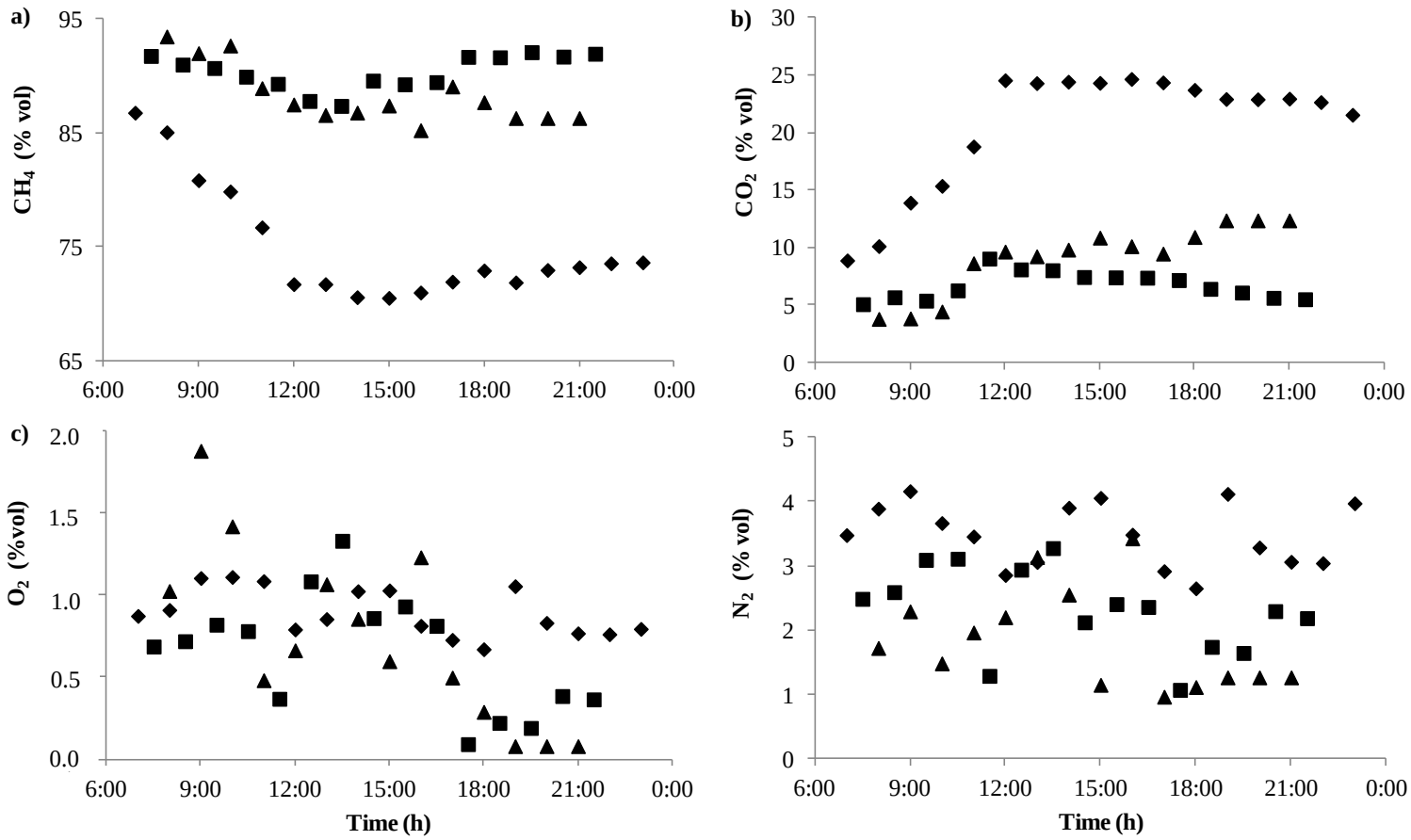

Figure
Click here to download Figure: Figure 4.docx

Figure 4. Time course of the concentration of (a) CH_4, (b) CO_2, (c) O_2 and (d) N_2 in the upgraded biogas at L / G ratios of 0.5 (♦), 1 (□), 2 (▲) and 5 (○).

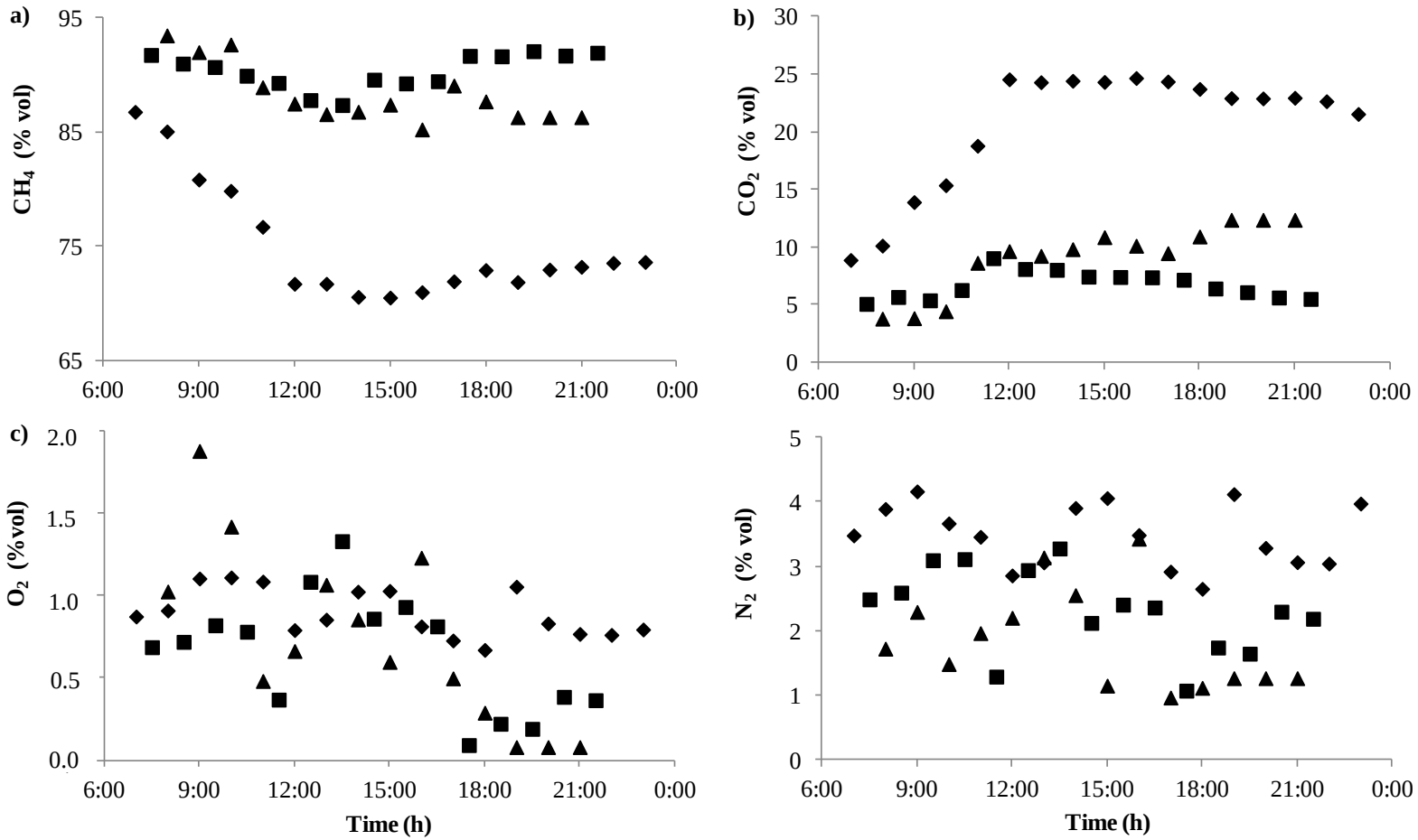

Figure
Click here to download Figure: Figure 5.docx

Figure 5. Time course of the influent (♦) and effluent (◊) concentrations of (a) TOC, (b) IC, (c) TN, (d) $N\text{-}NH_4^+$, (e) $N\text{-}NO_2^-$, (f) $N\text{-}NO_3^-$, (g) $P\text{-}PO_4^{3-}$ and (h) SO_4^{2-} throughout the three operational stages

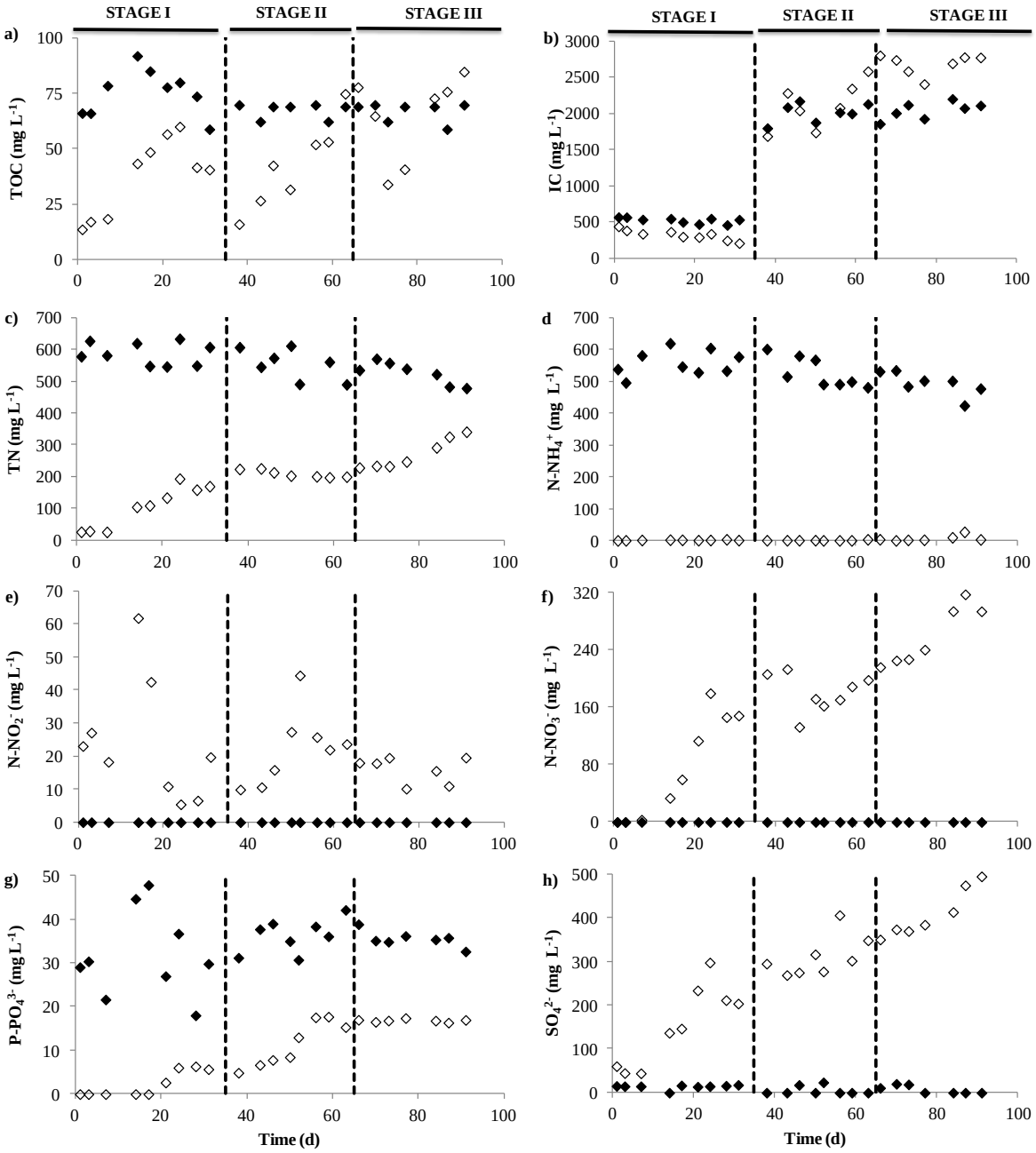

Figure
Click here to download Figure: Figure 6.docx

Figure 6. Time course of the structure of microalgae population in the HRAP: (■) *Chlorella* sp., (▩) *Pseudanabaena* sp. and (□) *Chloroidium saccharophilum*.

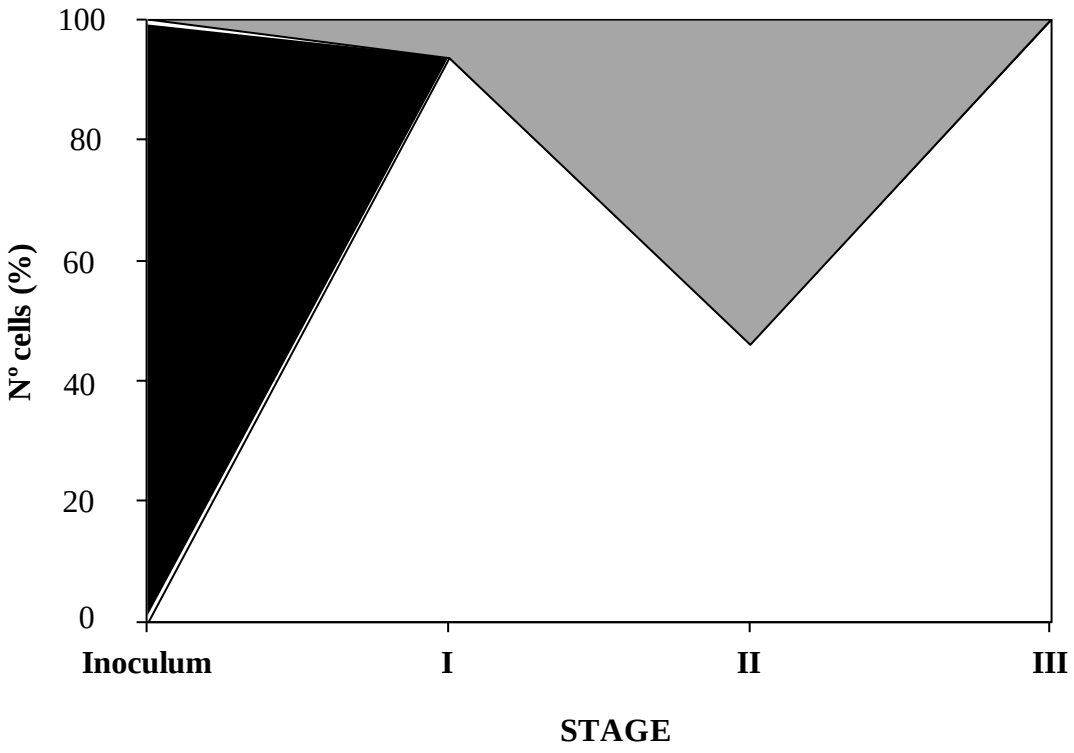

Table 1. Environmental and operational parameters during the three operational stages.

	STAGE		
PARAMETER	**I**	**II**	**III**
Date	05/07 - 08/08	09/08 – 06/09	07/09 – 04/10
Average temperature (ºC)	23.8 ± 6.7	23.5 ± 6.4	20.0 ± 6.7
Average PAR ($\mu mol\ m^{-2}\ s^{-1}$)	1427 ± 65	1258 ± 140	946 ± 174
Number of sun hours (h)	12 ± 1	11 ± 1	9 ± 1
$IC_{influent}$ ($mg\ L^{-1}$)	522 ± 40	2009 ± 135	2040 ± 120
Effluent from the settler ($L\ d^{-1}$)	0.6	0.8	No effluent

Table 2. Steady state removal efficiencies of total organic carbon, total inorganic carbon, total nitrogen, ammonium and phosphorus during the three operational stages.

STAGE	Removal efficiencies (%)				
	TOC	TIC	TN	$N\text{-}NH_4+$	$P\text{-}PO_4^{3-}$
I	74±7	95±1	86±4	100±0	92±2
II	57±6	72±8	87±4	100±0	84±5
III	59±7	75±7	80±8	99±1	85±5

Table 3. Carbon and nutrient recovery via biomass assimilation estimated from the carbon and nutrients removal, and the biomass elemental composition of the harvested biomass during stages I, II and III.

STAGE	Carbon and nutrient recovery as biomass (%)				Biomass elemental composition (%)			
	C	N	P	S	C	N	P	S
I	97±1	65±3	100±0	26±5	41.1	6.7	1.1	0.4
II	65±6	54±18	91±9	17±3	35.8	5.7	0.7	0.2
III	66±8	76±19	99±1	16±3	37.8	6.5	0.8	0.2

Electronic Annex

Click here to download Electronic Annex: Appendix.docx